JACS
JOURNAL OF THE AMERICAN CHEMICAL SOCIETY
Article
pubs.acs.org/JACS

Mechanistic Studies on the Metal-Free Activation of Dihydrogen by Antiaromatic Pentarylboroles

Adrian Y. Houghton,[†] Virve A. Karttunen,[‡] Cheng Fan,[†] Warren E. Piers,*[,†] and Heikki M. Tuononen*[,‡]

[†]Department of Chemistry, University of Calgary, 2500 University Drive NW, Calgary, Alberta, Canada T2N 1N4
[‡]Department of Chemistry, University of Jyväskylä, P.O. Box 35, FI-40014 Jyväskylä, Finland

Supporting Information

ABSTRACT: The perfluoro- and perprotiopentaphenylboroles **1** and **2** react with dihydrogen to effect H−H bond cleavage and formation of boracyclopentene products. The mechanism of this reaction has been studied experimentally through evaluation of the kinetic properties of the slower reaction between **2** and H_2. The reaction is first-order in both [borole] and [H_2] with activation parameters of $\Delta H^{‡}$ = 34(8) kJ/mol and $\Delta S^{‡}$ = −146(25) J mol^{-1} K^{-1}. A minimal kinetic isotope effect of 1.10(5) was observed, suggesting an asynchronous geometry for H−H cleavage in the rate-limiting transition state. To explain the stereochemistry of the observed products, a ring-opening/ring-closing mechanism is proposed and supported by the separate synthesis of a proposed intermediate and its observed conversion to product. Furthermore, extensive DFT mapping of the reaction mechanism supports the plausibility of this proposal. The study illustrates a new mechanism for the activation of H_2 by a strong main group Lewis acid in the absence of an external base, a process driven in part by the antiaromaticity of the borole rings in **1** and **2**.

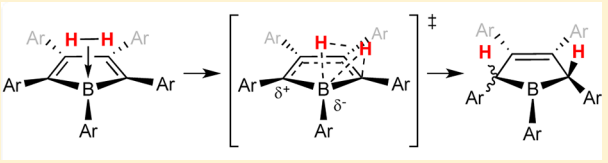

INTRODUCTION

Despite the low polarity and high bond strength of the H−H bond in dihydrogen, its activation is remarkably facile in the presence of transition metal compounds via oxidative addition,[1,2] σ-bond metathesis,[3,4] and electrophilic 1,2 addition type mechanisms.[5,6] Thus, the catalytic addition of H_2 to a variety of unsaturated organic functions and the hydrogenolysis of many M−X bonds are well known and understood phenomena that are widely deployed reactions in the chemical industry.[7]

While transition metal catalyzed hydrogen utilization is of tremendous economic and practical importance, transition metals and their complexes can be costly, and toxicity issues can also present challenges. Therefore, there has been significant interest in "metal-free" processes that do not require transition metals to activate and deliver hydrogen to substrates of interest.[8] Main group element based compounds that cleave hydrogen are less common, but a growing body of literature, beginning with the seminal discoveries of Power et al.,[9] suggest that main group elements can also cleave dihydrogen via low-energy pathways that synergistically depopulate the H−H σ bonding orbital while populating the H−H σ^* antibonding orbital. For example, Bertrand and co-workers showed[10] that stable singlet carbenes react rapidly with H_2 via a mechanism that is heterolytic in character but involves polarization of the H−H bond by donation of carbene electrons into its σ^* orbital and transfer of hydride to the carbene carbon. In both the Power and Bertrand systems, application to catalytic hydrogenation is limited by the lack of reversibility in the hydrogen cleavage reaction.

In 2006, Stephan and co-workers found[11] that sterically bulky Lewis acids combined with likewise sterically endowed Lewis bases are capable of activating H_2—reversibly—with remarkably low barriers. The acids are almost invariably perfluoroaryl boranes of high Lewis acid strength, but wide variation in the nature of the Lewis base is possible, and there are now many examples of this phenomenon in the literature.[12] The mechanism by which these systems polarize the H−H bond has been probed in the seminal $B(C_6F_5)_3/PR_3$ (R = mesityl, ^{t}Bu) systems both experimentally[13,14] and computationally,[15−17] and it is currently believed that a preformed "encounter complex", held together by weak van der Waals interactions, creates a pocket in which the H_2 can bind; the electric field created by the empty orbital on the boron and the filled orbital on phosphorus splits the H−H bond heterolytically with a very low barrier.[17] No experimental evidence for this encounter complex has yet been found, but the computational support for this picture is convincing for this particular system.

For bases with less symmetry complementarity, like imines[18] or carbenes,[19] similar encounter complexes have been described *in silico* but are somewhat less favored than those found for the borane/phosphine complexes. Thus, alternate mechanisms might be operative in these systems. For example, in a mechanism reminiscent of that proposed for $B(C_6F_5)_3$-catalyzed hydrosilation reactions,[20−24] the highly Lewis acidic borane might bind hydrogen via the σ bonding electrons; the base may then deprotonate the coordinated H_2 to generate the

Received: December 4, 2012
Published: December 21, 2012

ACS Publications © 2012 American Chemical Society

dx.doi.org/10.1021/ja311842r | J. Am. Chem. Soc. 2013, 135, 941−947

ion pair that is the product of dihydrogen activation. This process resembles the binding and deprotonation of dihydrogen to transition metal complexes.[25−27]

In this context, then, our observation that the *very* highly Lewis acidic perfluoropentaphenylborole[28] complex reacts essentially instantly with dihydrogen[29] to form the *cis* and *trans* isomers of the pentaarylboracyclopentenes is significant. With no external base present, it seems clear that the H_2 must interact with the boron center in some fashion in order that this reaction proceeds. In our initial report, we speculated that H_2 binding to the boron atom of the borole was followed by ring-opening to a 1-bora-pentadiene that then gave the observed *cis* and *trans* products via an electrocyclic ring closure and 1,2 hydride migration process.[30,31] Herein we present an experimental and computational study of this mechanism, using both the fully fluorinated system **1** and its unfluorinated pentaphenylborole[32,33] analogue **2**.

RESULTS AND DISCUSSION

Activation of H_2 by Pentaarylboroles. Reaction of the pentaarylboroles **1** and **2** with 1 atm of dihydrogen in methylene chloride occurs rapidly in the case of fully fluorinated **1**, and over the course of 4−5 h with the less Lewis acidic **2**, to yield the 1-bora-3-cyclopentene products **3** and **4**, respectively (Scheme 1).[29] The reactions are

Scheme 1

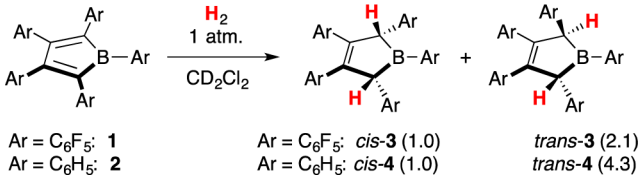

accompanied by a striking color change from the deep blue or purple colors of the boroles[34] to light yellow as the cyclic borane products are formed. The nature of the isomers **3** was determined by a combination of ^{1}H NMR spectroscopy and X-ray crystallography of the borapentenes themselves and their pyridine adducts. Although no structures have been determined, the unfluorinated isomers of **4** exhibited chemical and spectral behavior similar to that observed for **3**, and *trans*-**4**, as well as its pyridine adduct, were isolated analytically pure.

In both reactions, the *trans* isomer is favored; the numbers in parentheses in Scheme 1 indicate the relative amounts of each isomer under these ambient conditions. This ratio is a kinetic ratio and does not change upon heating the mixture to higher temperatures (50−80 °C). Interestingly, solid samples of **1** also react with H_2 to give the products, but under these conditions, the *cis* isomer of **3** is favored, being produced in a 10:1 ratio relative to the *trans* isomer. Irradiation of solutions of **3** thusly enriched in the *cis* isomer at 254 nm results in complete conversion to *trans*-**3** after about 4 days. Therefore, the *trans* isomer is also the thermodynamically most favored isomer in these systems, a notion supported by DFT calculations (see below).

Proposed Mechanism. The reaction of boroles **1** and **2** has been probed mechanistically via kinetic studies, the separate generation of a key intermediate and demonstration that it proceeds to products, and DFT studies. A mechanism that is consistent with these investigations is shown in Scheme 2. The first step entails reversible formation of a borole dihydrogen adduct (**I**). This step is faster for the more Lewis acidic perfluorinated borole **1** and accounts for the qualitatively much faster rates of reaction of **1** with H_2 in comparison to that observed for **2**. Attempts to observe these H_2 adducts met with failure; solubility issues thwarted the examination of solutions of either **1** or **2** under H_2 at low temperatures. At ambient temperatures, addition of the coordinated H_2 across an intra-ring B−C bond (step ***b***) produced the reactive zwitterionic intermediate *cis*-**II**, which features a carbocationic center that is stabilized by virtue of the fact that it is both benzylic and allylic; the adjacent borate center is probably also a stabilizing

Scheme 2

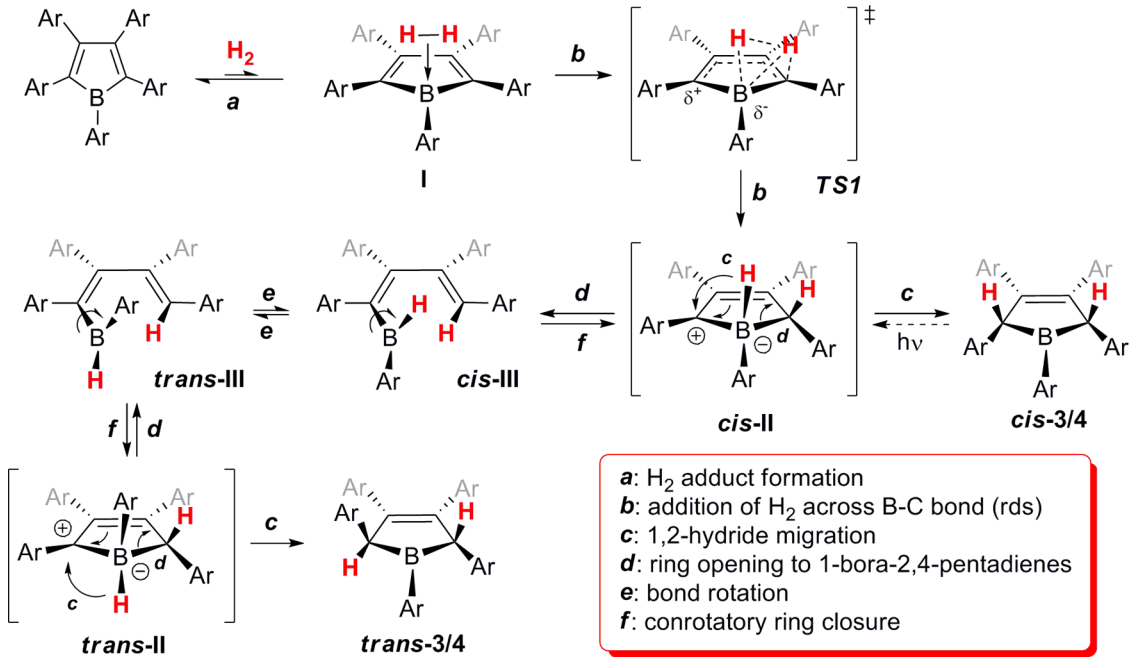

dx.doi.org/10.1021/ja311842r | J. Am. Chem. Soc. 2013, 135, 941−947

influence. Again, this intermediate is not observed directly, due to low-energy decomposition pathways that lead either directly to the *cis* isomers of the product 1-bora-3-cyclopentenes as indicated by step ***c*** or to an interconverting pair of 1-bora-2,4-pentadienyl rotamers (*cis/trans*-**III**) via a B−C bond-cleaving ring-opening, step ***d***. Note that this is the only path by which the *trans* isomers of **3** and **4** can form, since path ***c*** leads only to the *cis* isomers; path ***d*** must therefore be kinetically competitive with the seemingly more straightforward migration of hydride from *cis*-**II** to give *cis*-**3**/**4**. The rotomers of **III** are in rapid exchange by rotation about the B−C single bond (step ***e***), and each leads to one of the product isomers by a rapid conrotatory ring closure back to the cyclic zwitterions *cis/trans*-**II** that lead to the observed products via 1,2-hydride migration.

Compound **1** reacts too rapidly with H_2 at temperatures at which it exhibits reasonable solubility in CD_2Cl_2 to follow by NMR spectroscopy. Fortunately, the less Lewis acidic borole **2** has no such limitations, and its reactivity with H_2 can be followed conveniently over the course of 3−6 h to >4 half-lives using ^{1}H NMR spectroscopy. Methodology similar to that reported by Parkin and co-workers[35] was employed. In a typical procedure, an NMR tube was charged with a CD_2Cl_2 solution containing **2** and mesitylene as an internal standard. After degassing, dry H_2 was admitted to a defined pressure and temperature and the reaction followed by recording spectra every 5−10 min; between data collection steps the sample was agitated to ensure that the solution remained saturated with H_2. The [H_2] in solution was measured from the signal at 4.61 ppm, with the assumption that 25% of the H_2 existed as para-hydrogen.[36] It should be noted that, while the measurements indicated that [H_2] in solution was roughly equal to [**2**], the total H_2 in the 2.7 mL NMR tube was in at least 10-fold excess of the total **2** (0.0080 mmol). This method therefore relied on the assumption that agitation of the sample would replenish the dissolved H_2 much faster than the rate of reaction. That every trial obeyed a pseudo-first-order rate law indicates that this is a valid assumption.

The proposed mechanism predicts that the reaction should be first-order in both [H_2] and [**2**]. Indeed, by varying the pressure of H_2 from ca. 1 to 4 atm (10−40 times the amount of **2**), the observed rate constant (k_{obs}) changed in direct proportion to [H_2] (Figure 1). The slope of this ln-vs-ln plot is 1.01, indicating the order in [H_2] to be 1; plots of k_{obs} vs [H_2]^n (n = 1, 2, Figure S1) showed that only the n = 1 plot was linear, with a slope of 0.12 s^{-1}. First-order behavior in [**2**] is evidenced by the fact that every reaction profile can be fitted to a pseudo-first-order plot. These results are consistent with the second-order formation of the H_2 adduct **I**, at least in the case of unfluorinated **2**.

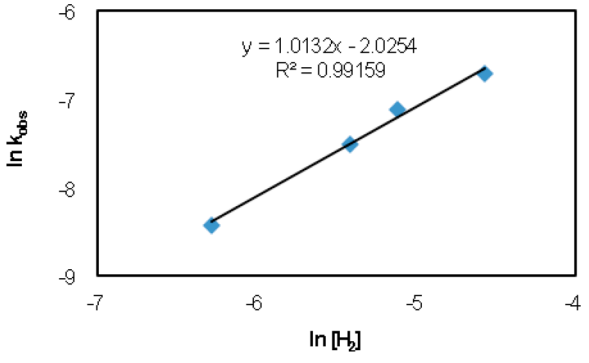

Figure 1. Plot of ln k_{obs} against ln [H_2] with [**2**] = 0.016 M under ca. 1−3.8 atm H_2 in CD_2Cl_2 at 293 K for the determination of the reaction order in [H_2] using the isolation method.

A kinetic isotope effect (KIE) for this reaction was measured by two methods. First, the ratio of k_{obs} values for the separate reaction of **2** with H_2 and D_2 showed a small effect of 1.10(5) (Figure 2). Second, exposure of **2** to a 1:1 mixture of H_2:D_2 resulted in a 1.1(1):1 ratio of *cis/trans*-**4** and d_2-*cis/trans*-**4** products, corroborating the result. The reaction of fully fluorinated **1** with a 1:1 mixture of H_2:D_2 gave a slightly larger KIE of 1.2(1). The small KIEs observed are consistent with binding of H_2 followed by a step (***b***, Scheme 2) in which the H−H bond is cleaved via an asynchronous transition state.

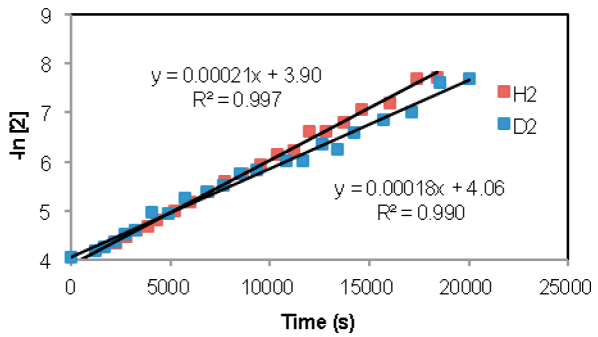

Figure 2. Pseudo-first-order plots of the reaction between **2** and H_2 (red) and D_2 (blue).

In a final set of kinetic experiments, the activation parameters for the reaction were derived from an Eyring plot (Figure 3):

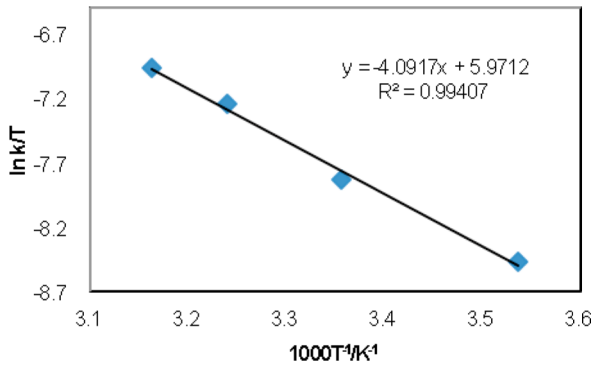

Figure 3. Eyring plot for the reaction of **2** (0.016 M) with H_2 (ca. 1 atm) in CD_2Cl_2 at 283, 298, 309, and 316 K.

$\Delta H^{\ddagger}$ = 34(8) kJ/mol and $\Delta S^{\ddagger}$ = −146(25) J mol^{-1} K^{-1}. Although the temperature range over which these measurements were conveniently made is quite narrow, the negative $\Delta S^{\ddagger}$ value is consistent with a bimolecular process. Using these activation parameters, the $\Delta G^{\ddagger}$ at 298 K is 78(16) kJ/mol.

While these kinetic experiments are consistent with the first steps in the proposed mechanism, the subsequent steps remain rather speculative. We thus sought to provide more evidence for the proposal through the separate synthesis of a 1-bora-2,4-pentadiene complex analogous to *cis*- or *trans*-**III**. Early attempts by Zweifel and co-workers[30,31] to generate such boranes led directly and rapidly to 1-bora-3-cyclopentenes analogous to products **3** and **4** herein, and so we have only succeeded in generating **III** (Ar = C_6H_5) *in situ*.

dx.doi.org/10.1021/ja311842r | J. Am. Chem. Soc. 2013, 135, 941−947

This was accomplished by the synthesis of the borinic ester **5** via the protic ring-opening of **2** by treatment with 1 equiv of phenol (Scheme 3). After exploring various hydroboration-based routes (as originally established by Zweifel), this proved the most convenient way to generate **5**. Of significance is the fact that the π-donating phenoxy group on boron in **5** stabilizes this compound toward ring-closing—so much so that **5** can be isolated as a pale yellow solid in 52% yield after recrystallization from hot toluene. The ^{11}B NMR spectrum of **5** contains a broad signal that appears at 44.8 ppm, which is comparable to that found for $Ph_2B(OMe)$ (45.2 ppm).[37] Furthermore, a crystal suitable for X-ray analysis was obtained by slow evaporation from dichloromethane; its molecular structure and selected metrical parameters are given in Figure 4.

Scheme 3

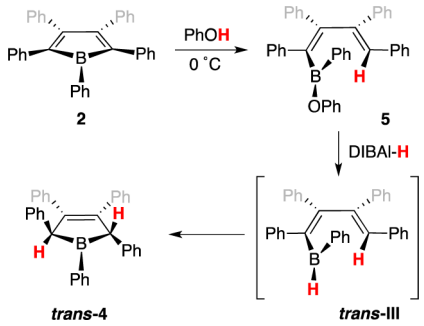

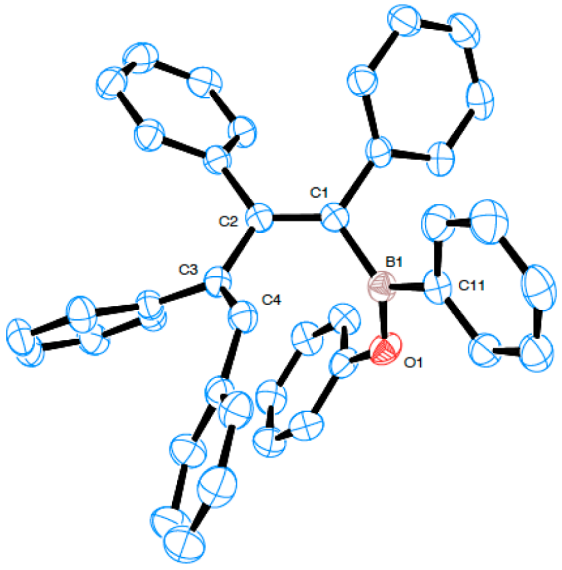

Figure 4. Thermal ellipsoid diagram (50%) of **5**. Selected bond lengths (Å) and angles (°): C1−C2 1.361(3), C2−C3 1.486(3), C3−C4 1.354(3), B1−C1 1.571(3), B1−O1 1.367(3), B1−C11 1.568(3); C1−B1−C11 122.05(17), C1−B1−O1 122.99(18), C11−B1−O1 114.76(17), and C1−C2−C3−C4 35.47.

Significantly, **5** adopts a cisoid 1-bora-2,4-pentadienyl geometry, which is required for the electrocylic cyclization to occur. Bond distances are as one would expect for localized double and single bonds; the short B1−O1 distance of 1.367(3) Å is indicative of strong π bonding in this linkage. The C1−C2−C3−C4 dihedral angle of 35.47(5)° orients the π bond between C3 and C4 toward the trigonal plane about B1; the nonbonding distance between C4 and B1 is only 2.79 Å.

As shown in Scheme 3, treatment of **5** with 1 equiv of DIBAl-H rapidly gave *trans*-**4** (exclusively), as evidenced by the emergence of the singlet at 4.85 ppm in the ^{1}H NMR spectrum characteristic of this compound. Addition of a few drops of pyridine resulted in the quantitative conversion to the pyridine adduct of *trans*-**4**. The spectroscopic signature of the compounds produced from **5** and DIBAl-H is identical to that from **2** and H_2 (Figure 5), with the exception that no evidence for the *cis* isomer of **4** is observed in the former reaction. While the reasons for this are not clear, it may reflect the fact that, in the H_2 reaction with **2**, the *cis* isomer arises exclusively via path ***c*** depicted in Scheme 2.

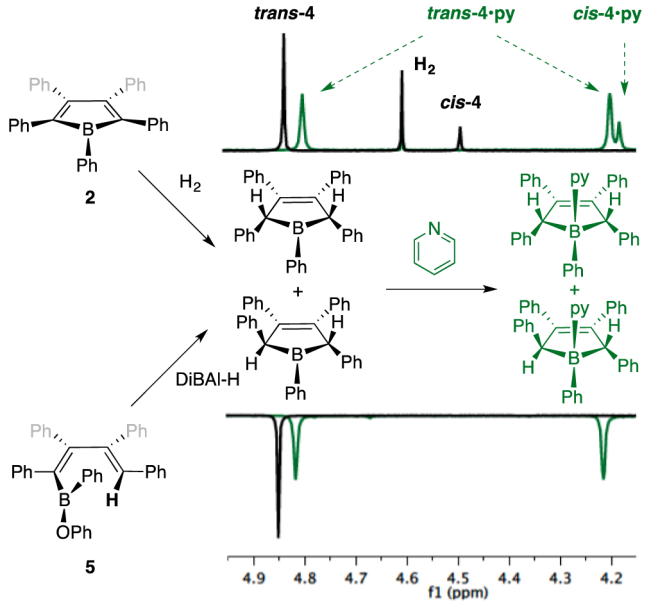

Figure 5. Comparison of the ^{1}H NMR of *trans*-**4** and the corresponding pyridine adduct *trans*-**4**-**py** generated from **2** and H_2 (top) and **5** and DIBAl-H (bottom).

These experimental studies provide convincing support for the mechanism proposed in Scheme 1, but the facility of these reactions and the limitations imposed by the physical properties of these sparingly soluble, highly Lewis acidic and reactive boroles necessarily dictate that aspects of the proposed mechanism remain experimentally opaque. Therefore, we turned to DFT calculations to probe the veracity of the overall mechanistic proposal and computed a complete energy surface for the reactions of both **1** and **2** with dihydrogen.

DFT Calculations. The mechanism outlined in Scheme 2 was examined in detail at the PBE1PBE/def-TZVP level of theory, employing the polarizable continuum model for the treatment of solvent effects (methylene chloride). The acquired solution-state energies are presented in Figure 6 for both the fluorinated (**1**) and unfluorinated (**2**) pentaphenylboroles.

The initial step on the reaction pathway is the reversible formation of a stable adduct (**I**) between the borole and a molecule of dihydrogen (step ***a*** in Scheme 2). This step is endergonic for both boroles, around 20 kJ/mol less so for the fully fluorinated system. Furthermore, the energy of the transition state (**TS0**) is virtually on par with that of the adduct. Consequently, these intermediates can release H_2 or access a transition state (**TS1**), leading to addition of H_2 across

dx.doi.org/10.1021/ja311842r | J. Am. Chem. Soc. 2013, 135, 941−947

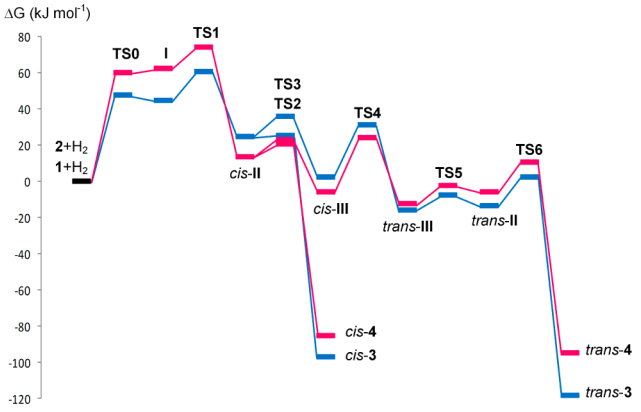

Figure 6. Calculated Gibbs free energies (kJ/mol) for the reaction of boroles **1** (blue) and **2** (red) with H_2.

an internal B−C bond to give intermediates *cis*-**II** (step ***b*** in Scheme 2). In this transformation, the π-electrons of the antiaromatic system function as an internal Lewis base, resulting in an overall heterolytic cleavage of the H−H bond. The energies for **TS1** are only 61 kJ/mol for **1** and 74 kJ/mol for **2**, in agreement with the experimentally observed reaction rates and the experimentally determined activation energy of 78(16) kJ/mol for borole **2**.

Continuing from the intermediates *cis*-**II**, the reactions can follow two alternate mechanisms whose transition states **TS2** and **TS3** have very similar energies. This indicates that both pathways are equally probable, in agreement with the observed formation of both *cis* and *trans* isomers. The transition states **TS2** and **TS3** are close in energy not only to each other but also to *cis*-**II**, which suggests that the intermediate is short-lived and that formation of intermediates *cis*-**II** is effectively irreversible.

The **TS2** involves a hydride transfer from boron to carbon (step ***c*** in Scheme 2) and leads to the formation of the *cis*-**3**/**4** products. However, the internal B−C bond lengths are significantly divergent in the *cis*-**II** structure: 1.566 vs 1.731 Å for the fluorinated system and 1.584 vs 1.711 Å in the phenyl-substituted borole. Consequently, **TS3** leads to B−C bond cleavage and ring-opening (step ***d***) to yield the *cis*-1-bora-2,4-pentadienyl rotamer (*cis*-**III**), which is the first intermediate on the pathway leading to products *trans*-**3**/**4**. The transformation of the *cis*-**III** rotamer to the corresponding *trans* isomer proceeds through **TS4** (step ***e***), with activation barriers of only 28 and 30 kJ/mol for boroles **1** and **2**, respectively. A subsequent, virtually barrierless (**TS5**) ring closure yields the *trans*-**II** intermediate (step ***f***), which readily undergoes hydride migration from boron to carbon (**TS6**, analogous to step ***c***) to give the *trans*-**3**/**4** products, thus completing the reaction pathway. In agreement with the photochemical experiments, the *trans*-**3** product is found to be more stable than the corresponding *cis* isomer for the fully fluorinated compound **1** (by 21 kJ/mol).[38]

As is evident from Figure 6, the relative energies of transition states **TS2**−**TS6** are significantly below that of the initial adduct **I** and the transition state of the rate-limiting step, **TS1**. Although the KIEs observed are quite small, the low concentration of adduct **I** and the highly asynchronous geometry for the H−H cleavage in **TS1** (Figure 7) are consistent with this observation. Indeed, in agreement with the KIE measurements, the reaction profiles shown in Figure 2

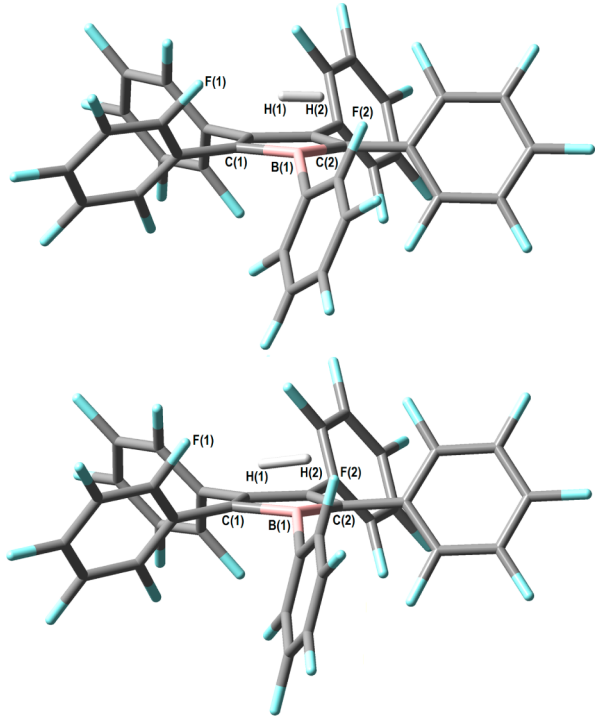

Figure 7. Computed structures for the H_2 adduct **I** for the fully fluorinated borole **1** (top) and the transition state **TS1** (bottom) for addition of H_2 across the internal B(1)−C(1) bond to form *cis*-**II**. Selected bond lengths (Å): (top) H(1)−H(2) 0.814, F(1)−H(1) 2.166, F(2)−H(2) 2.309, C(1)−H(1) 2.056, C(2)−H(2) 2.111, B(1)−H(1) 1.438, B(1)−H(2) 1.443; (bottom) H(1)−H(2) 1.057, F(1)−H(1) 2.266, F(2)−H(2) 2.391, C(1)−H(1) 1.450, C(2)−H(2) 2.142, B(1)−H(1) 1.328, B(1)−H(2) 1.304.

were found to be essentially independent of the isotope used in the calculations: substituting hydrogen in H_2 with deuterium had only a very minor (around 0−2 kJ/mol) effect on the relative Gibbs free energies calculated for both **I** and **TS1**.

A comparison of the two reaction profiles in Figure 6 shows that the overall energetics of the mechanism are largely independent of the identity of the borole, as in many steps the blue and red lines overlap or are otherwise very close to each other. The biggest differences between the two profiles are observed for the *trans*-**3**/**4** product as well as for the initial adduct **I** and the transition state **TS1**. In each of these cases, the fully fluorinated system is about 20 kJ/mol more stable than its phenyl analogue, suggesting that the difference in Gibbs energy could be related to the short F···H and F···B contacts observed in the optimized structures. This was examined by conducting calculations on boroles which had their phenyl substituents only partially fluorinated.

The calculations show that, for **1**, the structures **I** and **TS1** gain extra stabilization from two short F···H contacts (2.106−2.391 Å) that make an approximately 10 kJ/mol total contribution to their relative energies. Consequently, the first step on the reaction pathway is faster for the borole **1** not just because of its greater Lewis acidity but also because of the possibility to form van der Waals interactions that its phenyl-substituted analogue **2** inevitably lacks. In a similar fashion, the lower relative energy of *trans*-**3** compared to both *trans*-**4** and *cis*-**3** results in part from the two short F···B contacts (2.716 Å) in its structure. Selective F-to-H replacements showed that the combined effect of these interactions on the relative energy is 8

dx.doi.org/10.1021/ja311842r | J. Am. Chem. Soc. 2013, 135, 941−947

kJ/mol, which accounts for almost half of the difference between *trans*-**3** and *trans*-**4** structures.

As a whole, the results from theoretical calculations add considerable support for the pathway presented in Scheme 2. Nevertheless, in an effort to test the plausibility of alternate mechanistic possibilities, we performed a more comprehensive scan of the potential energy surfaces of **1** and **2** with H_2. As expected, the environment at and around the boron atom was found to be the single reactive site in both boroles. However, we were able to characterize an additional transition state in which H_2 adds to the external B−C bond involving the aromatic substituent bound to the boron center. Significantly, these transition states were found to be 72 and 46 kJ/mol higher in energy than the **TS1** of boroles **1** and **2**, respectively.[39] Furthermore, following the internal reaction coordinate toward products clearly showed that the characterized transition state leads to breakup of the B−C bond and subsequent formation of a borole with a B−H functionality and a molecule of benzene/pentafluorobenzene. Since neither ArH nor products arising from the highly reactive H-borole[34,40] were observed, this pathway is not competitive in the reaction of boroles with H_2.

■ CONCLUSIONS

The facile reaction of dihydrogen with antiaromatic boroles **1** and **2** illustrates that strongly Lewis acidic main group Lewis acids can bind hydrogen and activate it in the absence of an external Lewis base. Although dihydrogen adducts of Lewis acid centers incapable of π backbonding are ephemeral, these reactions show that, when a thermodynamic driving force is present, such adducts can lead to reactivity other than simple release of the bound H_2. Here, the antiaromaticity associated with the borole ring is a likely contributor to this driving force. For other Lewis acidic boranes, such as $B(C_6F_5)_3$, adducts with H_2 have been shown computationally to lie in energetic minima but are not thought to lie on the reaction coordinate for hydrogen splitting in the presence of a bulky trialkylphosphine Lewis base such as P^tBu_3. Little, however, is known regarding the mechanism of H_2 activation by $B(C_6F_5)_3$ in partnership with other, non-C_{3v}-symmetric Lewis bases. The role of H_2 adducts of boranes may be more pronounced in the mechanisms involving these systems.

The work described here suggests that an H_2 adduct of a pentaarylborole might be observable experimentally under the right conditions. Unfortunately, the solubility properties of **1** and **2** (particularly **1**) have precluded us from pursuing low-temperature spectroscopic studies. With solubilizing groups, such studies may yield interesting results; efforts along these lines are currently underway.

■ EXPERIMENTAL SECTION

General procedures are detailed in the Supporting Information.

Kinetics Experiments. A J. Young NMR tube was charged with a CD_2Cl_2 solution (0.5 mL) containing **2** (0.016 M) and mesitylene (0.004 M) as an internal standard. The solution was then subjected to three freeze−pump−thaw cycles and allowed to equilibrate at a given temperature. At this time H_2 gas was introduced and allowed to fill the tube for 2 min, taking care to not agitate it. The tube was carried to an NMR spectrometer in a dry ice/acetone bath and allowed to warm to the appropriate reaction temperature. Agitation of the tube was counted as $t = 0$. Spectra were recorded every 5−10 min using a delay of 45 s (~5 times T_1 for the methyl groups of mesitylene in CD_2Cl_2). For experiments at room temperature, a modified Kugelrohr apparatus was used to consistently agitate the samples between readings. The $[H_2]$ in solution was measured from the signal at 4.61 ppm, assuming a 3:1 ratio of *ortho* hydrogen:*para* hydrogen. The [**4**] in solution was measured from the allylic proton signals at 4.85 ppm (*trans*-**4**) and 4.50 ppm (*cis*-**4**) and from the aryl proton signals at 7.78 ppm (*trans*-**4**) and 7.68 ppm (*cis*-**4**). This was then used to infer the disappearance of product; hence the plots in the SI are shown as ln([**2**]). Activation parameters were determined by measuring rate constants at 10, 25, 31, and 43 °C, and agitation was achieved by inverting the NMR tube five times between readings. Higher pressures of H_2 were achieved by introducing H_2 at different temperatures: ~1 atm at 20 °C, ~1.5 atm at −72 °C (dry ice/acetone bath), ~2 atm at −130 °C (pentane/liquid N_2), and ~3.8 atm at −196 °C (liquid N_2).

Reactions with 1:1 H_2:D_2. Three J. Young NMR tubes were charged with a CD_2Cl_2 solution (0.5 mL) containing either **1** or **2** and toluene as an internal standard. The solutions were then subjected to three freeze−pump−thaw cycles and allowed to equilibrate to room temperature. To the first tube was added H_2. A 1:1 H_2:D_2 mixture was created by first placing both the vacuum and atmosphere lines under full (static) vacuum and then introducing H_2 (300 mmHg) followed by D_2 (300 mmHg) and letting the mixture equilibrate for a minimum of 4 h. The J. Young tube was then opened to allow the gas mixture in. This was then repeated with the third J. Young tube, adding D_2 to the vacuum line first, followed by H_2. All three tubes were agitated with a modified Kugelrohr apparatus overnight. The ^{1}H NMR spectra of each mixture were recorded, and the ratio of H_2:D_2 products was obtained by integration of appropriate signals.

Synthesis of 5. A solution of phenol (47 mg, 0.50 mmol) in dichloromethane (10 mL) was added to a cold (0 °C) solution of pentaphenylborole **2** (222 mg, 0.50 mmol) in dichloromethane (20 mL) via syringe over 30 min. The purple solution turned pale yellow almost immediately, and the ice bath was removed. After 30 min the volatiles were removed *in vacuo*, and yellow solid was recrystallized from hot toluene and washed with cold hexanes (2 × 3 mL). A pale yellow powder was obtained (140 mg, 52% yield). Crystals suitable for X-ray analysis were grown from slow evaporation from dichloromethane. ^{1}H NMR (400 MHz, CD_2Cl_2): δ = 7.90 (m, 2H, Ar_H), 7.41 (m, 1H, Ar_H), 7.33 (m, 2H, Ar_H), 7.19−6.87 (m, 20H, Ar_H + C═C-*H*), 6.83 (m, 2H, Ar_H), 6.76 (m, 2H, Ar_H), 6.70 (m, 2H, Ar_H). ^{13}C NMR (100 MHz, CD_2Cl_2): δ = 155.66, 152.88, 146.95, 145.64, 142.26, 139.31, 138.14, 136.70, 135.11, 131.98, 131.07, 130.80, 130.73, 130.55, 130.10, 129.08, 127.78, 127.69, 127.48, 127.40, 127.28, 127.08, 126.86, 126.48, 125.94, 123.20, 120.16. (Two peaks for the carbons bonded to boron were not observed due to the quadrupolar relaxation.) ^{11}B NMR (128 MHz, CD_2Cl_2): δ = 45(br). HRMS (TOF MS EI+): calcd for $C_{40}H_{31}BO$ 538.2468, found 538.2450.

Reaction of 5 with DiBAl-H and Pyridine. A solution of **5** 26 mg (0.050 mmol) in CD_2Cl_2 (~0.7 mL) was combined with DiBAl-H (50 uL, 1.0 M in hexanes) and shaken. After 20 min, two drops of pyridine was added to the NMR tube and the ^{1}H NMR spectrum recorded.

Reaction of 2 with H_2 and then Pyridine. In a J. Young NMR tube, a solution of **2** (5 mg, 0.01 mmol) in CD_2Cl_2 (~0.7 mL) was degassed at −78 °C and then charged with H_2 gas (ca. 1 atm). The tube was then rotated on a modified Kugelrohr apparatus for 10 h. Two drops of pyridine was added to the tube and the ^{1}H NMR spectrum recorded.

Computational Details. All calculations were done with the program packages Turbomole 6.3[41] and Gaussian09.[42] Geometries of the studied systems were optimized in the gas phase as well as in solution (methylene chloride) using the PBE1PBE density functional[43−46] in combination with Ahlrichs's TZVP basis sets.[47] The polarizable continuum model, as implemented in Gaussian 09, was used for the treatment of solvent effects.[48] The nature of stationary points found was assessed by calculating full Hessian matrices. To ensure that the calculated energetics are not significantly dependent on the employed basis set, the reaction profile of borole **1** was recalculated in the gas phase using Ahlrichs's def2-TZVPP basis sets.[49,50] Doubling the size of the basis sets resulted in only minor 1−10 kJ/mol changes to the relative energies. The program gOpenMol was used for all visualizations of molecular structures.[51,52]

dx.doi.org/10.1021/ja311842r | J. Am. Chem. Soc. 2013, 135, 941−947

■ ASSOCIATED CONTENT

Supporting Information

Crystallographic data files for **5** (CCDC 912008) as well as relative energies and .xyz coordinates of the calculated structures and complete ref 42. This material is available free of charge via the Internet at http://pubs.acs.org.

■ AUTHOR INFORMATION

Corresponding Author

wpiers@ucalgary.ca; heikki.m.tuononen@jyu.fi

Notes

The authors declare no competing financial interest.

■ ACKNOWLEDGMENTS

Funding for the experimental work described was provided by the Natural Sciences and Engineering Research Council of Canada in the form of a Discovery Grant to W.E.P. Funding for the computational work described was provided by the Academy of Finland and the Technology Industries of Finland Centennial Foundation in the form of a research grant to H.M.T. W.E.P. thanks the Canada Council for the Arts for a Killam Research Fellowship (2012-2014).

■ REFERENCES

(1) Vaska, L.; DiLuzio, J. W. *J. Am. Chem. Soc.* **1962**, *84*, 679−680.
(2) Johnson, C. E.; Eisenberg, R. *J. Am. Chem. Soc.* **1985**, *107*, 3148−3160.
(3) Watson, P. L.; Parshall, G. W. *Acc. Chem. Res.* **1985**, *18*, 51−56.
(4) Thompson, M. E.; Baxter, S. M.; Bulls, A. R.; Burger, B. J.; Nolan, M. C.; Santarsiero, B. D.; Schaefer, W. P.; Bercaw, J. E. *J. Am. Chem. Soc.* **1987**, *109*, 203−219.
(5) Fulmer, G. R.; Herndon, A. N.; Kaminsky, W.; Kemp, R. A.; Goldberg, K. I. *J. Am. Chem. Soc.* **2011**, *133*, 17713−17726.
(6) Burford, R. J.; Piers, W. E.; Parvez, M. *Organometallics* **2012**, *31*, 2949−2952.
(7) Hartwig, J. F. *Organotransition Metal Chemistry, from Bonding to Catalysis*; University Science Books: New York, 2010.
(8) Kenward, A. L.; Piers, W. E. *Angew. Chem., Int. Ed.* **2008**, *47*, 38−41.
(9) Spikes, G. H.; Fettinger, J. C.; Power, P. P. *J. Am. Chem. Soc.* **2005**, *127*, 12232−12233.
(10) Frey, G. D.; Lavallo, V.; Donnadieu, B.; Schoeller, W. W.; Bertrand, G. *Science* **2007**, *316*, 439−441.
(11) Welch, G. C.; Juan, R. R. S.; Masuda, J. D.; Stephan, D. W. *Science* **2006**, *314*, 1124−1126.
(12) Stephan, D. W.; Erker, G. *Angew. Chem., Int. Ed.* **2010**, *49*, 46−76.
(13) Piers, W. E.; Marwitz, A. J. V.; Mercier, L. G. *Inorg. Chem.* **2011**, *50*, 12252−12262.
(14) Marwitz, A. J. V.; Dutton, J. L.; Mercier, L. G.; Piers, W. E. *J. Am. Chem. Soc.* **2011**, *133*, 10026−10029.
(15) Rokob, T. A.; Hamza, A.; Stirling, A.; Soós, T.; Pápai, I. *Angew. Chem., Int. Ed.* **2008**, *47*, 2435−2438.
(16) Guo, Y.; Li, S. *Inorg. Chem.* **2008**, *47*, 6212−6219.
(17) Grimme, S.; Kruse, H.; Goerigk, L.; Erker, G. *Angew. Chem., Int. Ed.* **2010**, *49*, 1402−1405.
(18) Rokob, T. A.; Hamza, A.; Stirling, A.; Pápai, I. *J. Am. Chem. Soc.* **2009**, *131*, 2029−2036.
(19) Holschumacher, D.; Bannenberg, T.; Hrib, C. G.; Jones, P. G.; Tamm, M. *Angew. Chem., Int. Ed.* **2008**, *47*, 7428−7432.
(20) Parks, D. J.; Piers, W. E. *J. Am. Chem. Soc.* **1996**, *118*, 9440−9441.
(21) Parks, D. J.; Blackwell, J. M.; Piers, W. E. *J. Org. Chem.* **2000**, *65*, 3090−3098.
(22) Blackwell, J. M.; Sonmor, E. R.; Scoccitti, T.; Piers, W. E. *Org. Lett.* **2000**, *2*, 3921−3923.
(23) Rendler, S.; Oestreich, M. *Angew. Chem., Int. Ed.* **2008**, *47*, 5997−6000.
(24) Mewald, M.; Oestreich, M. *Chem.—Eur. J.* **2012**, *18*, 14079−14084.
(25) Kubas, G. J.; Ryan, R. R.; Swanson, B. I.; Vergamini, P. J.; Wasserman, H. J. *J. Am. Chem. Soc.* **1984**, *106*, 451−452.
(26) Heinekey, D. M.; Oldham, W. J. *Chem. Rev.* **1993**, *93*, 913−926.
(27) Jessop, P. G.; Morris, R. H. *Coord. Chem. Rev.* **1992**, *121*, 155−284.
(28) Fan, C.; Piers, W. E.; Parvez, M. *Angew. Chem., Int. Ed.* **2009**, *48*, 2955−2958.
(29) Fan, C.; Mercier, L. G.; Piers, W. E.; Tuononen, H. M.; Parvez, M. *J. Am. Chem. Soc.* **2010**, *132*, 9604−9606.
(30) Zweifel, G.; Clark, G. M.; Hancock, K. G. *J. Am. Chem. Soc.* **1971**, *93*, 1308−1309.
(31) Zweifel, G.; Backlund, S. J.; Leung, T. *J. Am. Chem. Soc.* **1977**, *99*, 5192−5194.
(32) Eisch, J. J.; Hota, N. K.; Kozima, S. *J. Am. Chem. Soc.* **1969**, *91*, 4575−4577.
(33) Braunschweig, H.; Fernández, I.; Frenking, G.; Kupfer, T. *Angew. Chem., Int. Ed.* **2008**, *47*, 1951−1954.
(34) Braunschweig, H.; Kupfer, T. *Chem. Commun.* **2011**, *47*, 10903−10914.
(35) Hascall, T.; Rabinovich, D.; Murphy, V. J.; Beachy, M. D.; Friesner, R. A.; Parkin, G. *J. Am. Chem. Soc.* **1999**, *121*, 11402−11417.
(36) Jacobsen, R. T; Penoncello, J. W. L., S. G.; Lemmon, E. W. *Int. J. Thermophys.* **2007**, *28*, 758−772.
(37) Jacob, P., III *J. Organomet. Chem.* **1978**, *156*, 101−110.
(38) For the unfluorinated system, *trans*-**4** is also the most stable (by 10 kJ/mol), but irradiation of *cis/trans*-**4** mixtures leads to extensive decomposition.
(39) Gao, S.; Wu, W.; Mo, Y. *Int. J. Quantum Chem.* **2011**, *111*, 3761−3775.
(40) Braunschweig, H.; Chiu, C.-W.; Kupfer, T.; Radacki, K. *Inorg. Chem.* **2011**, *50*, 4247−4249.
(41) *TURBOMOLE* V6.3, 2011; University of Karlsruhe and Forschungszentrum Karlsruhe GmbH, 1989−2007; TURBOMOLE GmbH, since 2007; available from http://www.turbomole.com.
(42) Frisch, M. J.; et al. *Gaussian 09*, Revision A.2; Gaussian Inc.: Wallingford, CT, 2009.
(43) Perdew, J. P.; Burke, K.; Ernzerhof, M. *Phys. Rev. Lett.* **1996**, *77*, 3865−3868.
(44) Perdew, J. P.; Ernzerhof, M.; Burke, K. *J. Chem. Phys.* **1996**, *105*, 9982−9985.
(45) Perdew, J. P.; Ernzerhof, M.; Burke, K. *Phys. Rev. Lett.* **1997**, *78*, 1396−1400.
(46) Adamo, C.; Barone, V. *J. Chem. Phys.* **1999**, *110*, 6185−6170.
(47) Schaefer, A.; Huber, C.; Ahlrichs, R. *J. Chem. Phys.* **1994**, *100*, 5829−5836.
(48) Tomasi, J.; Mennucci, B.; Cammi, R. *Chem. Rev.* **2005**, *105*, 2999−3094.
(49) Weigend, F.; Häser, M.; Patzelt, H.; Ahlrichs, R. *Chem. Phys. Lett.* **1998**, *294*, 143−152.
(50) Weigend, F.; Ahlrichs, R. *Phys. Chem. Chem. Phys.* **2005**, *7*, 3297−3305.
(51) Laaksonen, L. *J. Mol. Graphics* **1992**, *10*, 33−34.
(52) Bergman, D. L.; Laaksonen, L.; Laaksonen, A. *J. Mol. Graphics* **1997**, *15*, 301−306.